New approach to 3D inversion of MCSEM and MMT data using multinary model transform

Alexander V. Gribenko and Michael S. Zhdanov, University of Utah and TechnoImaging

SUMMARY

Marine controlled-source electromagnetic (MCSEM) surveys have become an important part of offshore hydrocarbon exploration. Magnetotelluric (MT) data are often also recorded by MCSEM receivers at almost no additional cost. In this paper we present a new approach to 3D inversion of MCSEM and MT data called multinary inversion. This method is based upon a transformation of the model parameters and their sensitivities from physical property space to a lithology-based space. In the case of marine EM problem, the multinary inversion exploits conductivity contrasts between different objects of the sea bottom, such as sediments and salt structures, or hydrocarbon and water-filled reservoirs. Our synthetic model study demonstrates that multinary inversion has potential application in the inversion of different types of marine EM data. For the models considered in the paper multinary approach provides better resolution than conventional inversion.

INTRODUCTION

Marine controlled-source electromagnetic (MCSEM) surveys have become intensively used for offshore petroleum exploration (Eidesmo et al., 2002; Carazzone et al., 2005; Hesthammer et al., 2010). EM receivers used in MCSEM surveys are also sensitive to magnetotelluric (MT) signals. Consideration of both data types can reduce the interpretation uncertainty. There are several joint 3-D inversion algorithms for both MCSEM and MT data interpretation(Mackie et al., 2007; Abubakar et al., 2009; Gribenko and Zhdanov, 2011).

Traditional inversion methods consider model parameters varying continuously within the known bounds. In some applications physical properties may be best described by a finite number of possible values which correspond to specific lithologies expected to be found in the area. Zhdanov and Cox (2013) introduced a deterministic method for directly inverting geophysical data to 3D lithological models. The method is general, and can be applied to any geophysical technique. It is based on a transformation of the model parameters and their sensitivities from the space with continuous distribution of the parameters to a discrete lithology-based space.

In this paper we include lithology-based model transform introduced by Cox et al. (2012) into our 3D joint MCSEM-MT inversion algorithm (Gribenko and Zhdanov, 2011). The multinary inversion method is tested on a synthetic model of the base of salt with a reservoir, and compared to the results of conventional inversions. These examples demonstrate that multinary inversion is a powerful tool, which can be applied to marine EM data inversion.

PROBLEM FORMULATION

In an MCSEM survey, sea bottom EM receivers record electric and magnetic fields arising from an electric bipole transmitter towed at some distance above the sea bottom. The same receivers can also record naturally occurring MT fields. The interpretation of magnetotelluric data is based on the calculation of the transfer functions between the horizontal components of the electric and magnetic fields, which form the MT impedance tensor (Zhdanov and Keller, 1994). We use the integral equation (IE) method to model the components of the EM field (Hohmann, 1975). In the case of MCSEM three-dimensional conductivity model is excited by an electromagnetic field generated by a horizontal electric bipole transmitter, while MT fields arise from a plane EM wave. It is well known that the EM field in such models can be presented as a sum of the background (normal) and anomalous fields:

$$\mathbf{E} = \mathbf{E}^b + \mathbf{E}^a, \;\; \mathbf{H} = \mathbf{H}^b + \mathbf{H}^a, \tag{1}$$

where the background field is a field generated by the given sources in the model with a background distribution of conductivity σ_b, and the anomalous field is produced by the anomalous conductivity distribution $\Delta\sigma(\mathbf{r})$, $\mathbf{r} \in V \subset R^3$. Then, the electric and magnetic fields can be obtained by the following integral expressions:

$$\mathbf{E}\left(\mathbf{r}'\right) = \int\int\int_V \mathbf{G}_E\left(\mathbf{r}',\mathbf{r}\right)\Delta\sigma\mathbf{E}\left(\mathbf{r}\right)dv + \mathbf{E}^b\left(\mathbf{r}'\right), \tag{2}$$

$$\mathbf{H}\left(\mathbf{r}'\right) = \int\int\int_V \mathbf{G}_H\left(\mathbf{r}',\mathbf{r}\right)\Delta\sigma\mathbf{E}\left(\mathbf{r}\right)dv + \mathbf{H}^b\left(\mathbf{r}'\right), \tag{3}$$

where $\mathbf{r}' \in P \subset R^3$, and $\mathbf{G}_E$ and $\mathbf{G}_H$ are electric and magnetic Green's tensors.

First, we find the electric fields inside the domain V where $\Delta\sigma \neq 0$. This requires the solution of a system of IE comprised of (2) formulated for the domain V. We use a contraction operator method to solve the IE system (Hursán and Zhdanov, 2002). Second, using (2) and (3) we calculate the EM fields in the receiver locations.

We can describe the forward problem by an operator equation:

$$\mathbf{d} = \mathbf{A}(\Delta\sigma), \tag{4}$$

where $\mathbf{d}$ is either MCSEM data vector comprised of the EM field components or MT impedances in the receivers. $\mathbf{A}$ is the nonlinear forward operator symbolizing the governing IE and MT transfer functions. Conventional inversion aims to solve operator equation (4) for three-dimensional anomalous conductivity distribution $\Delta\sigma$.

To solve ill-posed inverse problem (4) we use regularization theory (Tikhonov and Arsenin, 1977) based on minimization of the parametric (cost) functional:

$$P(\Delta\sigma) = \phi(\Delta\sigma) + \alpha S(\Delta\sigma) = min, \tag{5}$$

DOI http://dx.doi.org/10.1190/segam2013-0428.1

where $\phi(\Delta\sigma) = ||\mathbf{A}(\Delta\sigma) - \mathbf{d}||_2^2$ is the misfit functional between the predicted data $A(\mathbf{m})$ and the observed data $\mathbf{d}$, $S(\mathbf{m})$ is a stabilizing functional, and α is a regularization parameter. We minimize parametric functional using the re-weighted regularized conjugate-gradient (RRCG) method with adaptive regularization parameter selection (Zhdanov, 2002). To apply a gradient minimization technique it is necessary to calculate Fréchet derivative, sometimes called Jacobian or sensitivity matrix.

The Fréchet derivative in joint inversion is a combination of the MCSEM and MT data sensitivity matrices. Both the MT and MCSEM data derivatives contain Fréchet derivatives of the EM field components, which can be computed using the quasi-Born (QB) approximation (Gribenko and Zhdanov, 2007):

$$\mathbf{F}_{E,H}\left(\mathbf{r}_j \mid \mathbf{r}\right) = \widehat{\mathbf{G}}_{E,H}\left(\mathbf{r}_j \mid \mathbf{r}\right)\mathbf{E}^{(n)}\left(\mathbf{r}\right). \tag{6}$$

Note that the electric field $\mathbf{E}^{(n)}$ is computed using the rigorous IE forward modeling method during the predicted field computations. Therefore no extra forward modelings are required. To further reduce computational speed and computer memory requirements, we apply the footprint approach to the Fréchet derivative calculation (Cox et al., 2011). Once the sensitivities of the EM field components are found one can apply chain rule to find Fréchet derivatives of the MT impedances.

We used the joint MT-MCSEM inversion algorithm introduced by Gribenko and Zhdanov (2011). Joint inversion requires careful selection of relative data weighting (Commer and Newman, 2008) due to different resolutions of different data. We use an adaptive data weighting scheme as follows. Initial weights are selected as the inverse of the corresponding data error. As inversion progresses, data weights are allowed to change based on the convergence rate of the corresponding data.

Following Zhdanov and Cox (2013), we transform our physical properties m_i into a model space defined by a continuous range of so-called "multinary" model parameters $\widetilde{m}_i$ using a superposition of error functions:

$$\widetilde{m}_i = cm_i + \sum_{j=1}^{P} erf\left(\frac{m_i - m^{(j)}}{\sqrt{2}\sigma_j}\right), \tag{7}$$

where P is a total number of possible model parameter realizations or lithologies, $m^{(j)}$ is a physical value corresponding to lithology j, σ_j is a standard deviation of the value $m^{(j)}$, and c is a small constant used to avoid singularities in calculation of the derivatives of the multinary model parameters. All of the parameters in the formula (7) are chosen a priori, based on known geological information and common sense. Figure 1 (a) shows an example of transformation of the conductivity into multinary parameters. In this case two lithologies ($P = 2$) are present - sediments and seawater, with corresponding conductivities of 1 and 3 S/m. We can use the chain rule to compute Fréchet derivative $\widetilde{\mathbf{F}}_{E,H}$ of the multinary parameters $\widetilde{m}_i$:

$$\widetilde{\mathbf{F}}_{E,H} = \mathbf{F}_{E,H}\left(\frac{\partial \widetilde{m}_i}{\partial m_i}\right)^{-1}, \tag{8}$$

where $\mathbf{F}_{E,H}$ is computed by (6). Differentiation of (7) yields:

$$\frac{\partial \widetilde{m}_i}{\partial m_i} = c + \sum_{j=1}^{P} \frac{1}{\sqrt{2\pi\sigma_j}} \exp\left(-\frac{\left(m_i - m^{(j)}\right)^2}{2\sigma_j^2}\right). \tag{9}$$

Figure 1 (b) shows the derivative of the multinary function $\widetilde{m}_i$ described above. Approximate representation (9) of multinary function (7) can be interpreted with a statistical analogy, where each summation term in (9) is a Gaussian function representing the probability density distribution of each discrete physical property m_i with a mean value $m^{(j)}$ and a standard deviation σ_j. Representation (7) can then be interpreted as a cumulative density function of the physical properties.

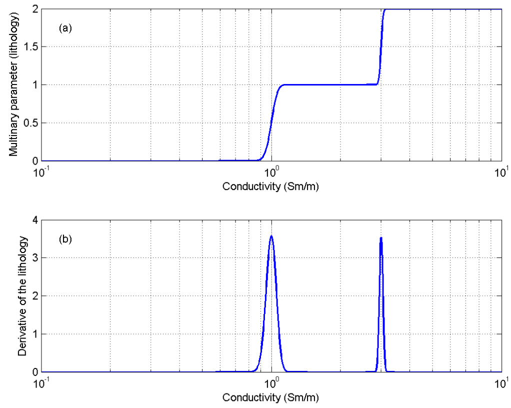

Figure 1: (a) - An example of transformation of the conductivity into multinary parameters. (b) - Derivative of the multinary function.

MODEL STUDY

As a base model for our study we consider the model proposed by Hoversten et al. (1998) to study subsalt resolution of MT data. Our 3D model is modified from its 2D prototype. We added a hydrocarbon reservoir to the model in order to test the inversion method with more then two lithologies present. First, we considered traditional separate inversions of the MT and MCSEM data, and joint inversion of MT and MCSEM data for continuous distribution of the conductivity. At the second stage, we applied the multinary inversion technique to the same datasets assuming the resistivities of the lithologies were the same as in the forward modeling.

Figures 2 and 3 show the vertical and horizontal sections of the Model, respectively. The model consists of 0.33 Ohm-m seawater and a 20 Ohm-m layer of salt embedded in a 1 Ohm-m layer of the sediments. To imitate realistic settings, the conductivities of the discretization cells were contaminated by 20% noise. The base of the salt layer has an uplift, which may be difficult to image correctly using seismic methods. The thickness of the salt layer varies from 400 m to 1 km, the seawater depth is 1 km, and the sediment layer is 1 km thick as well. The horizontal sections of Model 1 in Figure 3 also show

DOI http://dx.doi.org/10.1190/segam2013-0428.1

the locations of the receivers by the circles. The total number of 169 receivers was used for both the MT and MCSEM data. One MCSEM transmitter line was assumed running along the X axis from -10 to 10 km. The receivers are located 5 m above the sea bottom, and the transmitter is being towed 50 m above the sea bottom. The principal MT impedances at 12 frequencies, logarithmically spaced between 0.001 and 1 Hz were used as the MT data, and the in-line field component at 0.25 Hz was measured in the MCSEM survey.

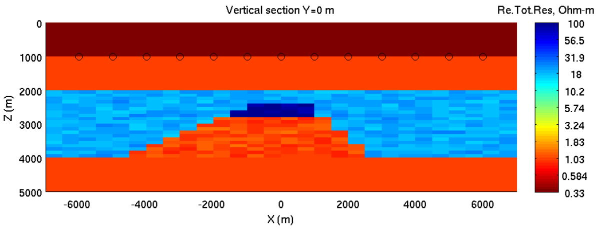

Figure 2: Vertical section of Model 1. Receivers are shown by circles.

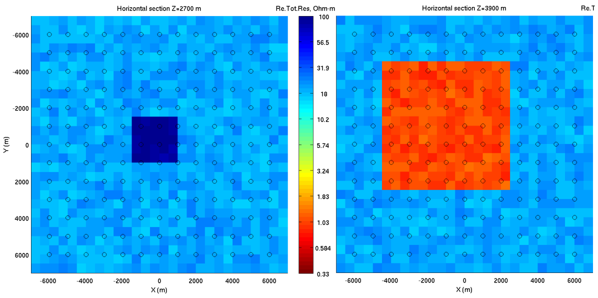

Figure 3: Horisontal sections of true Model 1. A 2700 m depth section is shown on the left and 3900 m is shown on the right. Receivers are shown by circles.

Figure 4 is the vertical sections of the inverse model obtained from the MT data. The conductive uplift in the base of the salt represents a good target for MT, and the inversion does a good job recovering the uplift. It may be difficult, however, to pinpoint the exact location of the boundary between the salt and the bottom sediments. Figure 5 shows the result of inversion of the MCSEM data. An increased resistivity zone corresponding to the reservoir is obvious. Due to sensitivity limitations, the vertical location and the shape of the reservoir are not well recovered. The conductive anomaly is not a perfect target for MCSEM, nevertheless, the inversion hints at the uplift with increased conductivity zone in the approximate location of the uplift. Figure 6 show the result of the joint MT-MCSEM data inversion. Note that, the result of MT data inversion was used as the initial and a priori model. Both anomalies - a sediment uplift and a reservoir - are clearly present in the joint inversion result.

In the next set of inversion experiments, we applied the newly developed multinary inversion to the same data. Three possible lithologies were allowed - sediments, salt, and reservoir.

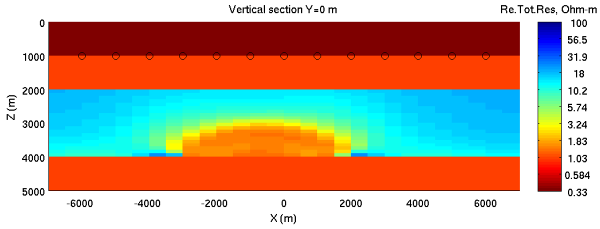

Figure 4: The vertical section through the result of the conventional inversion of MT data.

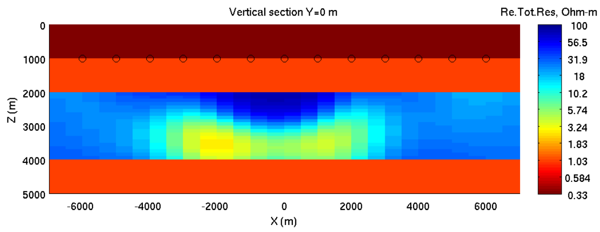

Figure 5: The vertical section through the result of the conventional inversion of MCSEM data.

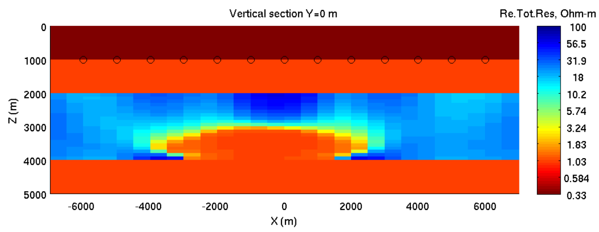

Figure 6: The vertical section through the result of the conventional joint inversion of MCSEM and MT data.

DOI http://dx.doi.org/10.1190/segam2013-0428.1

The corresponding expected resistivity values were set to the ones used in the forward modeling – 1, 20, and 100 Ohm-m, respectively. Figure 7 shows the vertical section of the MT inversion result. One can see that the sharp boundary between the sediments and the bottom of the salt is recovered with high accuracy. Note that, no indication of the reservoir is obvious from the MT inversion result alone. Figure 8 presents the result of the multinary inversion of the MCSEM data. The reservoir is clearly visible in the vertical section, however, its depth is underestimated. The accurate size detection may be quite helpful for reserve estimates in real situation. Figure 9 shows the result of joint multinary MT-MCSEM data inversion. The result of conventional joint inversion (Figure 6) was used as an initial model for the multinary joint inversion. Both anomalies - the sediment uplift and the reservoir - are clearly present in the joint inversion result. There is apparent separation between the sediment uplift and the reservoir, which may be due to the poor sensitivity to the depth of the reservoir or specifics of the multinary inversion. The observed and predicted data were matched to less then 1% normalized misfit.

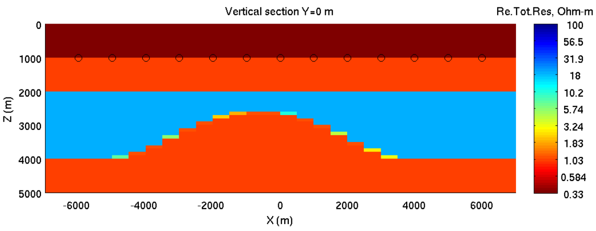

Figure 7: The vertical section through the result of the multinary inversion of MT data.

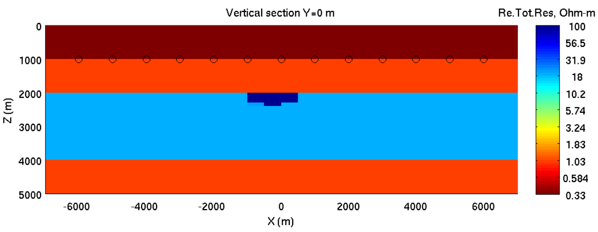

Figure 8: The vertical section through the result of the multinary inversion of MCSEM data.

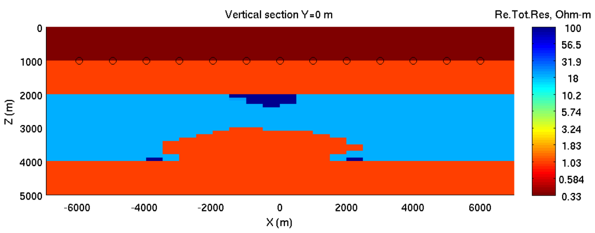

Figure 9: The vertical section through the result of the multinary joint inversion of MCSEM and MT data.

CONCLUSIONS

We have examined the feasibility of the joint multinary inversion of MCSEM and MT data for offshore HC reservoir detection. The method was tested on a model with three different lithology types: sea-bottom sediments, salt, and the HC reservoir. The results of our modeling study demonstrated that multinary inversion could recover the shapes of the true anomalies with high accuracy. The method is robust to geological noise. The joint inversion of MCSEM and MT data requires a good initial model and an appropriate weighting scheme. Future research will be focused on the variations of the conductivities of the lithologies.

ACKNOWLEDGMENTS

The authors acknowledge the support of the University of Utah Consortium for Electromagnetic Modeling and Inversion (CEMI) and TechnoImaging.

DOI http://dx.doi.org/10.1190/segam2013-0428.1

http://dx.doi.org/10.1190/segam2013-0428.1

EDITED REFERENCES

Note: This reference list is a copy-edited version of the reference list submitted by the author. Reference lists for the 2013 SEG Technical Program Expanded Abstracts have been copy edited so that references provided with the online metadata for each paper will achieve a high degree of linking to cited sources that appear on the Web.

REFERENCES

Abubakar, A., M. Li, J. Liu, and T. M. Habashy, 2009, Simultaneous joint inversion of MT and CSEM data using a multiplicative cost function: 79th Annual International Meeting, SEG, Expanded Abstracts, 719–723.

Carazzone, J. J., O. M. Burtz, K. E. Green, D. A. Pavlov, and C. Xia, 2005, Three-dimensional imaging of marine CSEM data: 75th Annual International Meeting, SEG, Expanded Abstracts, 575–578.

Commer, M., and G. A. Newman, 2008, New advances in three-dimensional controlled-source electromagnetic inversion: Geophysical Journal International, **172**, 513–535, http://dx.doi.org/10.1111/j.1365-246X.2007.03663.x.

Cox, L. H., G. A. Wilson, and M. S. Zhdanov, 2010, 3D inversion of airborne electromagnetic data using a moving footprint: Exploration Geophysics, **41**, no. 4, 250–259, http://dx.doi.org/10.1071/EG10003.

Cox, L. H., G. A. Wilson, and M. S. Zhdanov, 2012, 3D lithological inversion of geophysical data: 82nd Annual International Meeting, SEG, Expanded Abstracts, doi:10.1190/segam2012-0753.1.

Eidesmo, T., S. Ellingsrud, L. M. MacGregor, S. Constable, M. C. Sinha, S. Johansen, F. N. Kong, and H. Westerdahl, 2002, Sea bed logging (SBL), a new method for remote and direct identification of hydrocarbon filled layers in deepwater areas: First Break, **20**, no. 3, 144–152.

Gribenko, A., and M. S. Zhdanov, 2007, Rigorous 3D inversion of marine CSEM data based on the integral equation method: Geophysics, **72**, no. 2, WA73–WA84, http://dx.doi.org/10.1190/1.2435712.

Gribenko, A. V., and M. S. Zhdanov, 2011, Joint 3D inversion of marine CSEM and MT data: 81st Annual International Meeting, SEG, Expanded Abstracts, 552–556.

Hesthammer, J., A. Stefatos, S. Fanavoll, and J. Danielsen, 2010, The performance of CSEM as a de-risking tool in oil and gas exploration: 80th Annual International Meeting, SEG, Expanded Abstracts, 675–679.

Hohmann, G. W., 1975, Three-dimensional induced polarization and electromagnetic modeling: Geophysics, **40**, 309–324, http://dx.doi.org/10.1190/1.1440527.

Hoversten, M., F. Morrison, and S. Constable, 1998, Marine magnetotellurics for petroleum exploration, Part II: Numerical analysis of subsalt resolution: Geophysics, **63**, 826–840, http://dx.doi.org/10.1190/1.1444394.

Hursan, G., and M. S. Zhdanov, 2002, Contraction integral equation method in three-dimensional electromagnetic modeling: Radio Science, **37**, no. 6, doi:10.1029/200IRS002513.

Mackie, R., M. D. Watts, and W. Rodi, 2007, Joint 3D inversion of marine CSEM and MT data: 77th Annual International Meeting, SEG, Expanded Abstracts, 574–578.

Tikhonov, A. N., and V. Y. Arsenin, 1977, Solution of ill-posed problems: Winston & Sons.

Zhdanov, M. S., 2002, Geophysical inverse theory and regularization problems: Elsevier.

Zhdanov, M. S., and L. H. Cox, 2013, Multinary inversion for tunnel detection: Geoscience and Remote Sensing, **10**, no. 5, 1100–1103.

Zhdanov, M. S., and G. V. Keller, 1994, The geoelectrical methods in geophysical exploration: Elsevier.

DOI http://dx.doi.org/10.1190/segam2013-0428.1